26th EPS Conf. on Contr. Fusion and Plasma Physics, Maastricht, 14 - 18 June 1999 ECA Vol.23J (1999) 1481 - 1484

SIMULATION OF CARBON PELLET INJECTION AND IMPURITY CLOUD EXPANSION SCENARIOS IN STELLARATOR W7-AS BY MEANS OF A QUASI-THREE-DIMENSIONAL PELLET CODE

A. Ushakov*, L. Ledl, G. Veres**, R. Burhenn, R. Schneider, and L. Lengyel

Max-Planck-Institut für Plasmaphysik, EURATOM Association, D-85748 Garching
* St. Petersburg State Technical University, 195251 St. Petersburg, Russia
** KFKI Central Research Institute for Particle and Nuclear Physics, H-1525, Budapest, Hungary

Fourteen randomly selected C pellet injection scenarios were analyzed with the help of a quasi-3-D code. Three different ECR-heated discharges were considered: 9 shots in discharges with presumably Maxwellian energy distributions of the plasma particles (7 discharges with a magnetic field configuration having its maximum at the ECRH launching plane and 2 discharges with electron cyclotron current drive, Group 'A', see Table 1), and 5 'standard' discharges with ECR heating at a local B field minimum and the possible presence of non-thermal particles (Group 'B' in Table 1). The ranges of central discharge temperatures and densities were:
$2.3 \leq T_{e0}(keV) \leq 5.5$, $1.6 \leq n_{e0}(10^{19} m^{-3}) \leq 2.7$ ('thermal' discharges, group 'A'); and
$1.2 \leq T_{e0}(keV) \leq 1.7$, $3.6 \leq n_{e0}(10^{19} m^{-3}) \leq 7.0$ ('standard' discharges, 'B').
The pellet radii were close to 0.20 mm in all cases. The pellet velocities varied between 200 and 370 m/s. In the majority of the experiments, the velocities were around 300 m/s. The uncertainties of the measured pellet velocities were as follows: $\pm 15\%$ for discharges # 42991 and 42988, and $\pm 8\%$ for discharges # 43035 and 43143. In all other cases, the uncertainty is about 5%. In all cases, the pellet material was assumed to be homogeneous.

The computational model described in [1] and used in the present calculations substantially differs from the known neutral-gas-shielding ablation models and their derivatives. The early version of this model was checked against deuterium pellet scenario results in ASDEX Upgrade [2]. The results of neon pellet injection scenarios in ASDEX Upgrade were also successfully reproduced with the present version of this model [1].
The model of [1] consists of three modules: the first one calculates, at a sequence of radial positions, the local ionization and confinement radii of the pellet particles locally released, thus defining the channel cross-sections for the flux tubes in which the B-parallel expansion takes place. The second module calculates, based on the known energy distribution functions of the background plasma particles, the heating and expansion rates of the ablatant in the flux tube and the ablation rate itself. The third module calculates transfer quantities associated with advancing the pellet from flux tube to flux tube. The model includes radiation transport and loss calculations as well.
Possible drift of the pellet cloud with respect to the background plasma was not considered in the present calculations because of the following reasons: The magnitude of this drift depends on the characteristics of the polarization-induced currents and their loops in the background plasma [3] and is a complex time-dependent phenomenon. The drift velocity of an isolated plasmoid in a vacuum magnetic field can readily be estimated [4], but the same procedure cannot be applied to plasmoids surrounded by magnetically confined background plasmas. Although drift should be present in all scenarios in which grad($\mathbf{B}$) is present, no noticeable drift could be detected in the

carbon pellet experiments discussed here. Furthermore, not even all hydrogen pellet injection scenarios in tokamaks have shown the presence of drift [5]. Note: If plasma drift is present, collisions between the plasma particles and the neutrals surrounding the ablating pellet may also lead to a 'drift' of the neutral particles [6].

An elaborate non-equilibrium radiation model [7], supplemented by radiation transport calculations, has been applied. Since radiation transport is in reality 3-dimensional, the 1.5-D approximation applied here to the plasmoids expanding in the flux tubes is supplemented by an empirical factor accounting for radiation losses in the direction normal to the pellet path and lateral cloud surface (the vertical direction if the pellet path is restricted to the meridional plane). The optimization or adjustment of this factor, based on the analysis of numerous experimental scenario calculations, is yet to be done.

The computations were carried out on the basis of the measured (thermal) plasma temperature and plasma density distributions. The calculated and measured pellet penetration depths are compared in Table 1. In calculating the penetration depths, an effective plasma radius of 17 cm has been assumed. In the case of carbon pellets, the effective vaporization energy per particle depends upon the material properties of the pellets used. For the nine thermal (Maxwellian) discharge scenarios considered, an effective vaporization energy $\epsilon_{vap} = 3.5$ eV yielded optimum correspondence between the calculated and measured pellet lifetimes.

TABLE 1

(A.) Discharges with ECRH Injection at the locus of B = B_{max}.
Discharges presumably without non-thermal particles.

Disch.No.	l(measrd.)	l(calcld.)	Δl	Δ/l(measrd) %
43035	13.4 cm	15.2 cm	+1.8 cm	+13.
43045	13.4 cm	13.3 cm	- 0.1 cm	- 0.8
43010	11.4 cm	10.5 cm	- 0.9 cm	- 7.9
43006	10.3 cm	10.5 cm	+0.2 cm	+1.9
43004	10.4 cm	10.6 cm	+0.2 cm	+1.9
42995	10.2 cm	9.9 cm	- 0.3 cm	- 2.9
42994	10.7 cm	10.3 cm	- 0.4 cm	- 3.7
42991	9.5 cm	9.0 cm	- 0.5 cm	- 5.3
42988	14.0 cm	11.2 cm	- 2.8 cm	- 20.

(B.) 'Standard discharges' characterized by the presence of trapped particles.
As in the case of the previous 9 shots, Maxwellian energy distribution was assumed for the plasma particles also in these cases.

Disch.No.	l(measrd.)	l(calcld.)	Δl	Δ/l(measrd) %
43143	12.3 cm	15.9 cm	+3.6 cm	+29.
43565	19.5 cm	31.0 cm	+11.5 cm	+59.
43589	25.0 cm	29.5 cm	+4.5 cm	+18.
43580	18.0 cm	24.5 cm	+6.5 cm	+36.
43857	15.0 cm	19.0 cm	+4.0 cm	+27.

With regard to the first group of discharges with presumably Maxwellian thermal plasmas, Group 'A' in Table 1, the deviation between the calculated and measured penetration depths is, on the average, 6% (based on the absolute values), or notably less if the arithmetic mean of the deviations is calculated or the uncertainties associated with the pellet velocities are taken into account.

In Fig.1, three calculated quantities - the local ablation rate, the radiation power locally emitted, and the (e-folding) length of the CII(720nm) emission zones along the magnetic field lines

(associated with the plasmoids expanding in the succession of flux tubes) - upper, middle, and lower frames, respectively - are plotted as functions of the radial coordinate. For the purpose of comparison, the *measured* distributions of the CII(720nm) line emission (CCD signal, a.u.) are also shown in the same frames (dotted lines). Two representative discharges are considered: # 42995 and # 43006. The ablation rate and the radiation power are averaged over the residence time of the pellet in a flux tube, the calculated e-folding length is monitored at the end of this time.

The *measured* light emission signal shown was obtained from a two-dimensional time-integrated CCD image of the cloud by down-loading, line by line, the signals stored in the pixel arrays perpendicular to the direction of pellet motion. Note that the shape of this curve notably differs from the light emission curves observed in tokamaks: the CCD CII(720nm) signal recorded is almost symmetric with respect to the pellet 'midlifetime' and is characterized by approximately equal rise and decay times, although the pellet moves in the direction of increasing plasma temperatures. In tokamak discharges, maximum emission is usually observed shortly before the end of the pellet lifetime.

In the upper frame, the calculated local ablation rate (solid line) is compared with the distribution of the measured CCD signal. A notable spatial shift between the maxima of the two curves is observed.

In the middle frame, the spatial distribution of the radiation power - total power and CII(720nm) line radiation - emitted by the carbon plasmoids confined by and expanding in the succession of flux tubes along the magnetic field lines (solid line) is shown. Again, a notable shift between the maxima of the calculated and measured light emission distributions can be observed.

On the other hand, no spatial shift can be observed between the maxima of the calculated ablation rate and light emission curves (compare the curves in the upper and middle frames).

In the lower-frame figures, the calculated e-folding lengths of the CII(720nm) line emission zones along the magnetic field lines monitored at the end of the residence times (solid line) are plotted and compared with the measured CCD signal. As can be seen, no spatial shift exists between these two lines. The e-folding lengths deducable from the time-integrated CCD image are of the order of 1 to 2 cm and remain approximately constant along the pellet path.

As has been noted, the computational model was validated with the help of earlier hydrogen and neon pellet injection scenarios [1,2]. Assuming that both the basic assumptions used in the computational model and the experimental data supplied as input for the scenario calculations (the effective coordiates of the pellet trajectory and the associated plasma parameters, etc.) are correct, the shift between the calculated and measured CII(720nm) emision curves, or that between the ablation rate and measured light emission distributions, may be due to the following phenomena:

(a) The CCD curves displayed stem from time-integrated signals whereas the calculated curves correspond to certain time instants.

(b) The presence of nonthermal (energetic) plasma particles in the outer plasma regions would shift the locus of maximum particle deposition toward the plasma boundary. However, the penetration depths of the first nine pellets could very well be reproduced on the basis of the assumption of Maxwellian background plasmas.

(c) The presence of an outward directed drift of the pellet cloud across the magnetic field would also explain the shift observed. However, the photographic diagnostics performed [8] showed no evidence of shift.

The cause of the symmetry of the measured CII(720nm) emission pattern as well as the shift between the measured and calculated emission signals require further investigation. In any case, care should be exercized by interpreting radiation emission intensities in terms of local ablation rates, or possible shifts between these curves in terms of drifts.

Considering the five 'standard' discharges, Group 'B' in Table 1, a systematic deviation between the measured and the predicted penetration depths can be observed: the calculated penetration depths are, on the average, 33% larger than the measured ones. The cause of this notable deviation is most likely the presence of non-thermal particles in the 'standard' discharges. One of the assumptions used in the computational model was the existence of a single-temperature thermal background plasma with the same Maxwellian energy distribution function for the trapped and passing particles, i.e. the absence of non-thermal particles. This assumption was apparently violated. Since no information was available on the flux and energy of the non-thermal particles, their effect could not be taken into account in the computations.

REFERENCES

[1] Lengyel, L., Büchl, K., Pautasso, G., Ledl, L., Ushakov, A., Kalvin, S., and Veres, G., paper to appear in Nucl. Fusion (manuscript accepted: February 1999).
[2] Spathis, P., and Lengyel, L., Nucl. Fusion **34** (1994), 675.
[3] Lengyel, L., Plasma Phys. Control. Fusion **9** (1997), 647.
[4] Lengyel, L., Nucl. Fusion **17** (1977), 805.
[5] Houlberg, W., private communication (Garching, April 1999).
[6] Kristof, G., and Lengyel, L., Phys. Plasmas **5** (1998), 315.
[7] Veres, G., and Lengyel, L., J. Nucl. Materials **250** (1997), 96.
[8] Ledl, L., et al., 'Carbon Pellet Injection Scenarios...', paper presented at this conference.

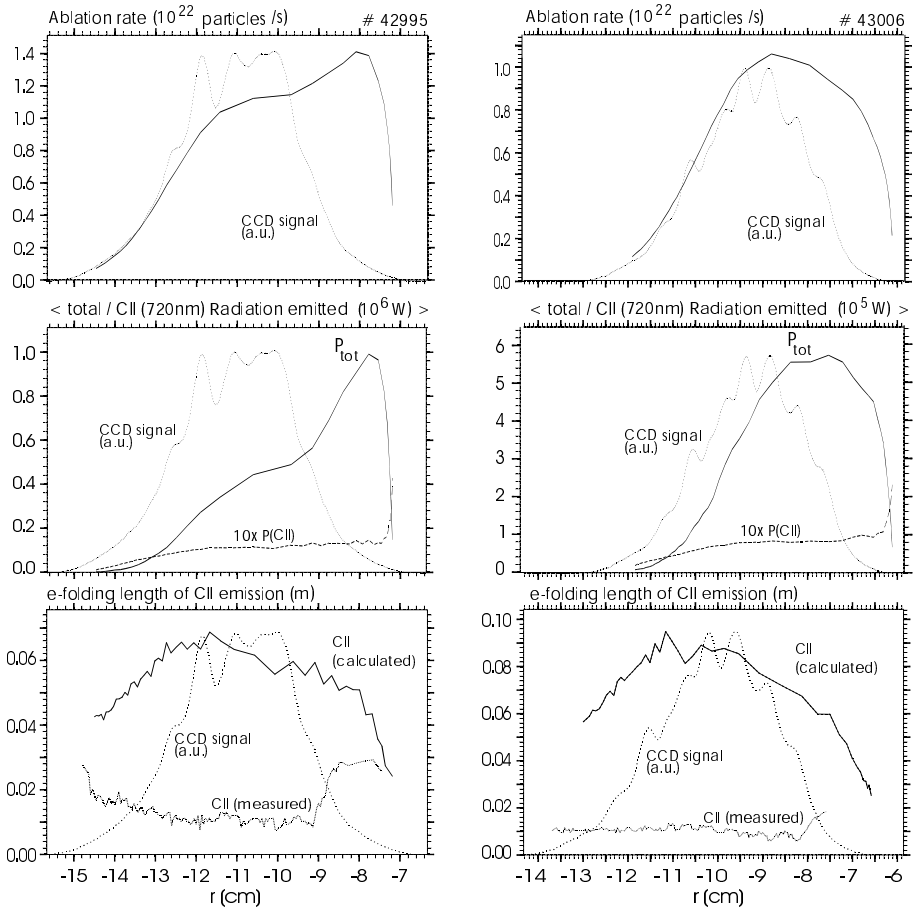

Figure 1: Comparison of ablation characteristics calculated along the pellet path with measured CII emission (dotted lines) for two pellet injection scenarios: shots # 42995 and # 43006.